AGU ADVANCING EARTH AND SPACE SCIENCES

Geophysical Research Letters®

RESEARCH LETTER
10.1029/2023GL104732

Dissolved Organic Radiocarbon in the West Indian Ocean

Ellen R. M. Druffel[1], Christian B. Lewis[1,2], Sheila Griffin[1], Alessandra Flaherty[1,3], Megha Rudresh[4], Niels E. Hauksson[1], Robert M. Key[5], Ann P. McNichol[6], Jeomshik Hwang[7], and Brett D. Walker[8]

[1]Department of Earth System Science, University of California, Irvine, CA, USA, [2]National Isotope Centre, GNS Science, Lower Hutt, New Zealand, [3]Division of Geological and Planetary Sciences, California Institute of Technology, Pasadena, CA, USA, [4]Department of Marine Geology and Geochemistry, University of Hawai'i-Manoa, Manoa, HI, USA, [5]Atmospheric and Oceanic Sciences Program, Princeton University, Princeton, NJ, USA, [6]Woods Hole Oceanographic Institution, Woods Hole, MA, USA, [7]School of Earth and Environmental Sciences, Seoul National University, Seoul, Korea, [8]Department of Earth and Environmental Science, University of Ottawa, Ottawa, ON, Canada

Key Points:

- ^{14}C aging of deep dissolved organic carbon (DOC) northward is not similar to that of deep dissolved inorganic carbon, showing that transport of deep water is not the main control of ^{14}C in DOC
- Variability of deep DOC ^{14}C indicates heterogeneity in the DOC pool, perhaps by dissolution of surface-derived, particulate organic C
- Low DOC $\delta^{13}C$ in deep water from two stations may suggest a source of chemosynthetically produced organic matter

Supporting Information:

Supporting Information may be found in the online version of this article.

Correspondence to:

E. R. M. Druffel,
edruffel@uci.edu

Citation:

Druffel, E. R. M., Lewis, C. B., Griffin, S., Flaherty, A., Rudresh, M., Hauksson, N. E., et al. (2023). Dissolved organic radiocarbon in the West Indian Ocean. *Geophysical Research Letters*, *50*, e2023GL104732. https://doi.org/10.1029/2023GL104732

Received 7 JUN 2023
Accepted 11 SEP 2023

Author Contributions:

Conceptualization: Ellen R. M. Druffel, Brett D. Walker
Data curation: Ellen R. M. Druffel, Sheila Griffin, Robert M. Key, Brett D. Walker
Formal analysis: Ellen R. M. Druffel, Sheila Griffin, Niels E. Hauksson, Robert M. Key, Jeomshik Hwang, Brett D. Walker
Funding acquisition: Ellen R. M. Druffel
Investigation: Robert M. Key, Brett D. Walker

Abstract We report marine dissolved organic carbon (DOC) concentrations, and DOC $\Delta^{14}C$ and $\delta^{13}C$ in seawater collected from the West Indian Ocean during the GO-SHIP I07N cruise in 2018. We find bomb ^{14}C in DOC from the upper 1,000 m of the water column. There is no significant change in $\Delta^{14}C$ of DOC in deep water northward, unlike that of dissolved inorganic carbon (DIC), suggesting that transport of deep water northward is not controlling the ^{14}C age of DOC. Variability of DOC $\Delta^{14}C$, including high values in the deep waters, is more pronounced than in other oceans, suggesting that dissolution of surface derived particulate organic carbon is a source of modern carbon to deep DOC in the West Indian Ocean. Low $\delta^{13}C$ are present at two of the five stations studied, suggesting a source of low $\delta^{13}C$ DOC, or additional microbial utilization of deep DOC.

Plain Language Summary Dissolved organic carbon (DOC) is the most abundant pool of organic carbon in ocean water. It is thought to form primarily from photosynthetic organisms in surface waters, however the radiocarbon (^{14}C) ages of DOC in the Atlantic and Pacific oceans are 4,900–6,400 years old. We find aging of deep DOC in the West Indian Ocean is not similar to that for dissolved inorganic carbon, indicating that transport of deep water northward is not the main control of ^{14}C in DOC. Evidence of young DOC is observed in the deep Indian.

1. Introduction

Dissolved organic carbon (DOC) is the largest pool of organic carbon in the ocean. It is mainly produced by photosynthesis in the surface, and is altered or removed as CO_2 through microbial activity (Jiao et al., 2010), and photolysis (Mopper et al., 1991). Previous work has found significant correlation between the size, reactivity and ^{14}C age of DOC (Amon & Benner, 1996; Benner & Amon, 2015; Kaiser & Benner, 2009; B. W. Walker et al., 2016). Other sources of DOC include riverine input, chemoautotrophy at high and low temperature hydrothermal systems (Lang et al., 2006; McCarthy et al., 2011), as well as graphite input (Estes et al., 2019) to deep seawater.

Radiocarbon (^{14}C) is produced in the stratosphere by cosmic ray secondaries (neutrons) bombarding atmospheric nitrogen atoms, and is quickly oxidized and mixed into the troposphere as $^{14}CO_2$. Beginning in the late 1950s, ^{14}C-dating of marine dissolved inorganic carbon (DIC) was used to measure transit time of deep waters in the world ocean. Broecker et al. (1960) found that DIC in deep North Atlantic water was ~800 ^{14}C years old, and Bien et al. (1965) reported deep North Pacific water was ~2,200 ^{14}C years old, revealing a transit time for the deep ocean conveyor of approximately ~1,400 years. Using DIC ^{14}C measurements made during the global GEochemical Ocean SECtions Study, Stuiver et al. (1983) reported that the replacement times for Pacific, Atlantic and Indian ocean deep waters were ~510, 275, and 250 years, respectively.

Radiocarbon in marine DOC of ocean water is much older than that of DIC, ranging from ~4,900 ^{14}C years in the deep North Atlantic (Druffel et al., 2016) to ~6,400 ^{14}C years in the North Pacific (Beaupré & Druffel, 2009), a difference of 1,500 ^{14}C years, similar to that for DIC. Transit times of DOC in the deep central and east Pacific northward are similar to those of DIC (Druffel et al., 2021), indicating that both DOC and DIC undergo similar ^{14}C aging as bottom and deep waters flow northward.

Methodology: Ellen R. M. Druffel, Christian B. Lewis, Sheila Griffin, Alessandra Flaherty, Megha Rudresh
Project Administration: Ellen R. M. Druffel
Resources: Christian B. Lewis, Sheila Griffin, Alessandra Flaherty
Software: Sheila Griffin, Robert M. Key
Supervision: Sheila Griffin
Validation: Ellen R. M. Druffel, Sheila Griffin, Ann P. McNichol, Brett D. Walker
Visualization: Robert M. Key
Writing – original draft: Ellen R. M. Druffel, Christian B. Lewis
Writing – review & editing: Ellen R. M. Druffel, Christian B. Lewis, Sheila Griffin, Niels E. Hauksson, Robert M. Key, Ann P. McNichol, Jeomshik Hwang, Brett D. Walker

The global ocean overturning circulation begins with formation of dense, cold waters at high latitudes that sink to deep depths in the North Atlantic and Southern Oceans. Deep waters flow toward lower latitudes, mixing with warmer, less dense waters above, transforming to warmer, less dense waters (Indian and Pacific deep waters) that return to the surface in the Southern Ocean (Stuiver et al., 1983; Talley, 2013; Toggweiler et al., 1989a, 1989b).

In the deep Indian Ocean, Srinivasan et al. (2000) used corrected DI^{14}C concentrations (adjusted for the addition of surface-derived, sinking particles) to estimate the mean upwelling transport of bottom water. They found faster upwelling in the West Indian Ocean than that further east due to the rough bottom topography in the west. Unlike the Pacific and Atlantic oceans, the Indian Ocean contains numerous, isolated basins, whose sills (2,500 m depth) prevent significant horizontal transport of deep water (Figure 1).

Bercovici et al. (2018) reported DOC ^{14}C measurements from the southeast Indian and Southern oceans (from 29°S to 56°S) and concluded that DOC Δ^{14}C are similar across water masses. For example, circumpolar deep water (CDW) and North Atlantic Deep Water (NADW) had DOC Δ^{14}C of $-491 \pm 13‰$ and $-481 \pm 8‰$, respectively.

The Indian Ocean is unique because of its undersea topography, circulation patterns, and permanent oxygen minimum zone (OMZ) to the North. Despite its importance, the Indian Ocean is understudied relative to other ocean basins. The focus of this work is to use DOC carbon isotopic signatures (Δ^{14}C and δ^{13}C) to study DOC cycling in the Indian Ocean. We show that DOC Δ^{14}C in deep water from the West Indian Ocean ranges from $-442‰$ to $-517‰$, with variability that is greater than that observed in the Pacific and Southern oceans (Druffel et al., 2019, 2021).

2. Collection and Methods

Seawater was collected from two legs of the GO-SHIP I07N cruise along 52°E–57°E from 29°S to 8°N aboard the NOAA Ship *Ronald H. Brown* (April–June 2018) (Figure 1, Table S1 in Supporting Information S1). Samples collected from five stations (3, 23, 47, 72, and 97) were analyzed for ^{14}C and ^{13}C and reported here (Druffel, 2023). Samples collected from two other stations (119 and 123) at 17°N and 18°N were lost due to a failed freezer. DOC samples shallower than 800 m were filtered using pre-combusted (500°C, 2 hr), GF/F (0.7 μm 70 mm diameter) filters into pre-combusted, 1 L Amber Boston Round glass bottles and capped with acid cleaned (10% HCl), polytetrafluorethylene (PTFE)-lined caps and PTFE sheet liners (cleaned in Chromerge). DOC samples were frozen at sea at −20°C.

In the lab, DOC samples were thawed by immersion in hot water and shaken to fully dissolve precipitated salt crystals (Beaupré et al., 2007; B. D. Walker et al., 2019). Samples were diluted with 18.2 MΩ Milli-Q water ([DOC] = 0.8 ± 0.3 μM), acidified with LCMS grade 85% phosphoric acid, and stripped of DIC with He gas (grade 5.0). Samples were UV oxidized to CO_2 for 4 hr in a quartz reactor and collected as described by Beaupré et al. (2007). DOC concentrations ([DOC]) were corrected for CO_2 loss due to breakthrough from the Horibe glass trap cooled with liquid nitrogen during collection (B. D. Walker et al., 2019). Uncertainty of [DOC] values were ±0.6 μM. The mass was quantified by integration using an infrared CO_2 gas analyzer (LI-COR Inc., model LI-6252) (B. D. Walker et al., 2019).

For Δ^{14}C measurements, samples were converted from CO_2 to graphite by reduction on iron catalyst using zinc (B. D. Walker & Xu, 2019; Xu et al., 2007). Radiocarbon measurements were made by us at the Keck Carbon Cycle AMS Laboratory at the University of California, Irvine (Santos et al., 2010). Radiocarbon results are reported as Δ^{14}C values that are corrected for date of collection according to convention (Stuiver & Polach, 1977). Total uncertainty of the Δ^{14}C analyses was ±4‰, the standard deviation of the differences between duplicate Δ^{14}C analyses of seawater from the same Niskin collections. There was one set of duplicate analyses run for each station. The δ^{13}C of each sample was measured on a split of the CO_2 produced from UV oxidation of the DOC sample using a Gas Bench II and Thermo Finnegan Delta Plus isotope ratio mass spectrometer, with a total uncertainty of ±0.2‰.

3. Results

3.1. DOC Concentrations

The concentrations of DOC were highest in the upper 50 m of the water column (69.2–76.8 μM; Figure S2 in Supporting Information S1 and Druffel, 2023). Concentrations decreased markedly between 83 m and 1,000 m

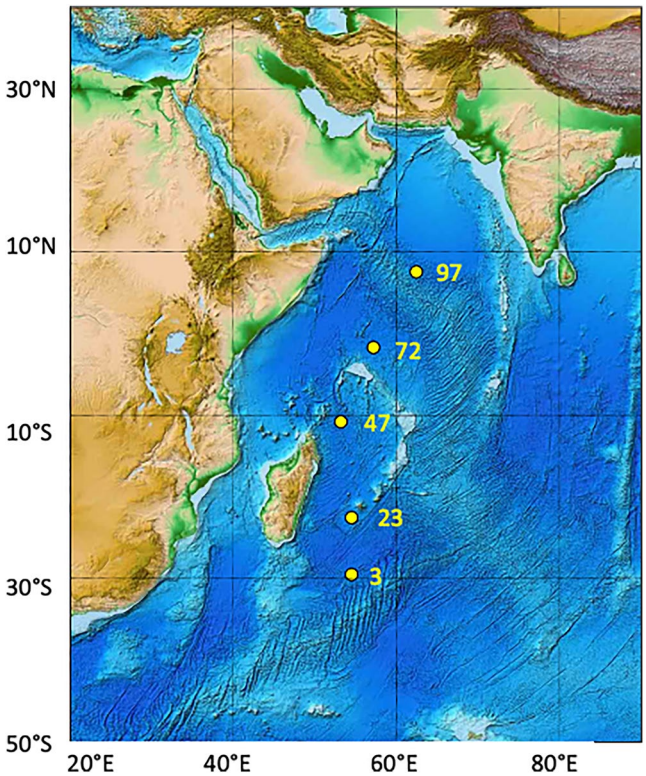

Figure 1. Map of stations sampled during the I07N cruise in the West Indian Ocean in April–June 2018. Dark blue regions indicate depths >3,000 m, and ridges and other areas <2,500 m depth are indicated by lighter shades of blue.

depth; values ranged from 64.2 to 41.0 μM. Average [DOC] below 1,000 m for all stations were similar within error, ranging from 39.3 ± 1.6 μM ($n = 7$) at stn 3 in the south, to 40.2 ± 0.3 μM ($n = 7$) at stn 97 in the north.

3.2. DOC $\Delta^{14}C$ Measurements

The DOC $\Delta^{14}C$ for surface samples (3–50 m depth) collected from the five I07N stations ranged from −244‰ (stn 3) to −227‰ (stn 23) (Figure 3a and Druffel, 2023). DOC $\Delta^{14}C$ values decreased with depth in the upper 1,060 m to lows ranging from −480‰ (stn 47) to −462‰ (stn 72) (Figure 2b, Druffel, 2023). Most DOC $\Delta^{14}C$ deeper than 1,060 m ranged from −505‰ (at stn 23 2,625 and 3,227 m) to −480‰ (stn 97 1,302 m) (Figure 2b). Note that the scales for the *x*-axes in Figures 2a and 2b are different. The lowest deep values were found at stn 97 (−513‰ at 3,000 m) and stn 72 (−517‰ at 2,601 m), and the highest deep values were found at stn 3 (−442‰ at 3,826 m) and stn 97 (−475‰ at 3,300 m).

3.3. DOC $\delta^{13}C$ Measurements

The DOC $\delta^{13}C$ ranged from −22.0‰ (stn 3) to −20.4‰ (stn 23) in the upper 1,060 m (Figure 3a and Druffel, 2023). Values were less variable below 1,060 m (Figure 3b). Station averages ranged from −21.3 ± 0.3‰ (stn 3 $n = 7$) to −21.1 ± 0.1‰ (stn 47 $n = 6$). The four lowest values (−22.0‰, −21.8‰, −21.8‰, and −22.0‰) were found at stn 3 at 414, 714, 3,826, and 4,467 m depth, respectively.

4. Discussion

The discussion is presented in four parts. First, the presence of bomb ^{14}C in DOC in the upper 1,000 m of the Indian Ocean water column is discussed. Second, we compare the ^{14}C aging of DOC in the deep Indian to that of DIC from previous cruises in CDW flowing northward. Third, we discuss the variability of the DOC $\Delta^{14}C$ and $\delta^{13}C$ in the deep Indian and its possible sources. Fourth, the relationship between surface DOC $\delta^{13}C$ and sea surface temperature (SST) is discussed.

4.1. DOC $\Delta^{14}C$ in Surface and Intermediate Water Masses

Bomb ^{14}C, produced in the late 1950s and early 1960s by thermonuclear weapons testing, is present in DIC (Stuiver & Ostlund, 1983) in the upper 1,000 m of the water column. Evidence of bomb ^{14}C in DOC in the upper 1,000 m of the water column has been shown (Cherrier et al., 1999; Williams & Druffel, 1987). The DOC in the North Pacific surface waters ($\Delta^{14}C = -146$) has been estimated to contain 44% old deep DOC (−520‰) and 56% surface bomb DOC (+150‰) (Williams & Druffel, 1987).

In our I07N surface samples (0–50 m), the highest DOC $\Delta^{14}C$ value (−227‰) is from 4 m depth at stn 23 (22°S) (Figure 2a and Druffel, 2023). Intermediate surface values (−236‰, −239‰, and −239‰) are from near-equatorial latitudes (10°S, 1°N, 8°N, respectively), where higher density water with lower $\Delta^{14}C$ waters intersect the sea surface. The lowest surface DOC $\Delta^{14}C$ was from stn 3 (−244‰, 29°S) where SST was lowest (23.1°C) and density was highest. These results are consistent with surface DOC $\Delta^{14}C$ from the East Pacific between 5°N (−206‰) and 25°S (−271‰) (Druffel et al., 2021) and the southeast Indian at 29°S (−227‰) (Bercovici et al., 2018). Using the Williams and Druffel (1987) mass balance calculation, the DOC in surface water at Stn 3 in the subtropical Indian Ocean ($\Delta^{14}C = -227$‰) is composed of 51% bomb DOC ($\Delta^{14}C = +25$‰ Hansmann and Sonnerup) and 49% deep DOC ($\Delta^{14}C = -487$‰) (Druffel, 2023). This is similar to the estimates made by Williams and Druffel (1987) for the North Pacific in 1985.

Subantarctic Mode Water (SAMW) is between 139 and 500 m in the West Indian Ocean at 29°S and 22°S (sigma theta 26.5–26.6), where salinity is high (Figure S1a in Supporting Information S1), and chlorofluorocarbon

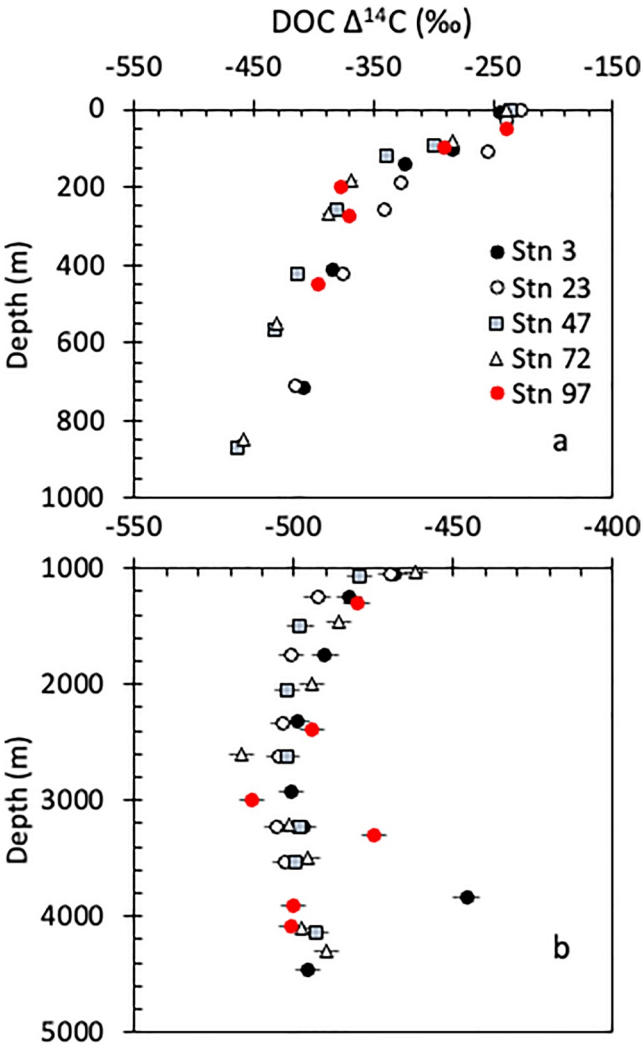

Figure 2. Dissolved organic carbon $\Delta^{14}C$ versus depth for samples collected on the I07N cruise in 2018 from (a) 0–1,000 m, and (b) 1,000–5,000 m depth. Latitudes for each station are: 29°S (Stn 3), 22°S (Stn 23), 10°S (Stn 47), 1°N (Stn 72), and 8°N (Stn 97).

(CFC-11) concentrations were 2.5–3.0 pmol/kg in 2018 (Figure S1c in Supporting Information S1) (Bullister, 2018). In SAMW, our DOC $\Delta^{14}C$ data at stn 3 (29°S) were −324‰ and −385‰ at 139 and 414 m, and at stn 23 (22°S) were −328‰, −342‰, and −376‰ at 191, 257, and 425 m, respectively.

Antarctic Intermediate Water (AAIW) in the West Indian is characterized by a minimum salinity (34.40–34.48 psu) (Figure S1a in Supporting Information S1). It is found between sigma-theta 27.1–27.3 and had CFC-11 concentrations of 1.5–3.0 pmol/kg in 2018 (Bullister, 2018) (see Figure S1c in Supporting Information S1). DOC $\Delta^{14}C$ in AAIW at stn 3 are −468‰ and −483‰ at 1,051 and 1,251 m, respectively. One sample at stn 23 (22°S 1,050 m) was AAIW (salinity 34.49 psu) and has a DOC $\Delta^{14}C$ of −470‰. Thus, samples from our two southernmost stations contained AAIW, and values were similar.

4.2. ^{14}C Aging of DOC and DIC in Circumpolar Deep Water and Input of Surface POC to the Deep Indian

DOC ^{14}C ages in CDW are calculated from DOC $\Delta^{14}C$ (^{14}C age = –ln(($\Delta^{14}C$ + 1,000)/1,000) × 8,033 years) for samples whose densities (sigma4) ranged from 45.75–45.80 (~2,400–3,900 m depth). Flow of NADW travels around South Africa and then northward on both sides of Madagascar (Mantyla & Reid, 1995), though the I07N cruise was north of this flow. The DOC ^{14}C ages in CDW are plotted versus latitude of collection for water samples (Figure 4a). The Model II geometric mean regression of DOC ^{14}C ages versus latitude shows an insignificant increase (35 ± 100 ^{14}C years) from 29°S to 8°N. Two DOC ^{14}C ages for samples from stn 3 (3,826 m 4,740 ^{14}C years) and stn 97 (3,300 m 5,180 ^{14}C years) were anomalous, having ^{14}C ages much younger than the other deep results and were not included in this analysis (see Section 4.3).

We compare DOC aging to DIC aging using measurements from past cruises that are plotted versus latitude (Figure 4b) (Key & Quay, 2002; Stuiver & Ostlund, 1983). The Model II geometric mean regression displays that an increase of the DIC ^{14}C age between 29°S (1,580 ± 10 ^{14}C years) and 8°N (1,690 ± 10 ^{14}C years) is 110 ± 20 ^{14}C years (Figure S2b in Supporting Information S1). Results for DIC ^{14}C ages of results from the I07N cruise in 2018 from NOSAMS (Hansmann & Sonnerup, 2022) (107 ± 40 ^{14}C years) (Figure 4c) are equivalent to those from the earlier DIC results.

Our analysis shows that DOC and DIC aging are dissimilar in CDW that flows northward in the West Indian Ocean. It is noted that the distance tracked is short (29°S to 8°N). Nonetheless, it appears that transport northward is not the primary control of DOC aging between these latitudes.

D. C. Smith et al. (1992) reported that hydrolytic enzyme activity on marine aggregates rapidly converts POC to DOC. It is conceivable that hydrolysis of modern POC from the surface produces DOC during transport to the deep Indian, causing deep DOC $\Delta^{14}C$ to be higher, thus counteracting the aging of DOC as water flows northward. To obtain aging of DOC similar to that of the DIC (110 ^{14}C years), $\Delta^{14}C$ of DOC at 8°N would need to decrease from −500‰ at 29°S to −507‰ at 8°N. This would require an input of 1% of surface POC with a $\Delta^{14}C$ of 25‰ (Hansmann & Sonnerup, 2022) to deep DOC with a $\Delta^{14}C$ of −507‰. Given that the average flux of organic C to the deep Northwest Indian (1,882 m depth) was ~11 gC/m^{-2}/yr in 1996 (S. L. Smith, 2001), and a standing stock of DOC in the water column of 1,900 gC (4,000 m depth), this would provide an input of 0.6% of the deep DOC per year ((11 gC/1,900 gC) × 100). This is of the same magnitude as the amount of surface POC required to dissolve to DOC in the deep ocean to counteract the aging of ^{14}C of deep DOC (1%), and thus offers a possible mechanism for maintaining the relatively high $\Delta^{14}C$ of DOC in the deep Northwest Indian Ocean.

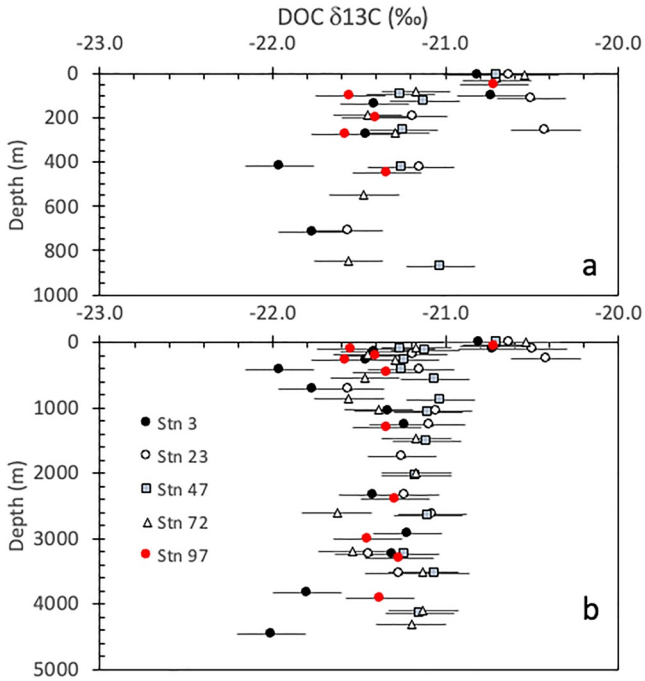

Figure 3. Dissolved organic carbon $\delta^{13}C$ versus depth for samples collected on the I07N cruise in 2018 from (a) 0–1,000 m, and (b) 1,000–5,000 m depth. Latitudes for each station are: 29°S (Stn 3), 22°S (Stn 23), 10°S (Stn 47), 1°N (Stn 72), and 8°N (Stn 97).

4.3. Possible Source(s) of DOC $\Delta^{14}C$ and $\delta^{13}C$ Variability

Most of the deep DOC $\Delta^{14}C$ between 2,600 and 4,000 m depth are comparable, with an average of −500 ± 3‰ (n = 12). There are four outlier values, from stn 3 (−442‰ 3,826 m), stn 97 (−475‰ 3,300 m, −513‰ 3,000 m), and stn 72 (−517‰ 2,601 m), that were not included in this average. In addition, there are four DOC $\delta^{13}C$ values from stn 3 (averaged −21.9 ± 0.1‰) that are lower than all other I07N results. Also, there are 5 results from Stn 72 that are lower than most other analyses (average −21.5 ± 0.1‰). The average for all other samples was −21.2 ± 0.3‰ (n = 55). All samples with outlier $\Delta^{14}C$ or $\delta^{13}C$ have [DOC] values within error of the average deep [DOC]. This suggests that either the cause of the isotopic outliers could be independent of [DOC] and within our analytical precision, or that some internal cycling of DOC is present at these locations (e.g., concomitant addition and removal of DOC while maintaining steady state [DOC]).

Reasons for isotopic variance in the deep DOC include: (a) the addition of DOC from either sinking POC or chemoautotrophic formation of DOC, (b) ^{14}C-free contamination (e.g., oil), and (c) input of chemosynthetic, low $\delta^{13}C$ DOC from hydrothermal ridges and flanks. First, all samples deeper than 800 m depth were not filtered prior to collection. The concentration of suspended POC in open ocean water is low, generally <0.2 μmol kg^{-1}, whereas [DOC] ranges from 39 to 43μmol kg^{-1}. It is possible that large, sinking particles were collected in the niskin bottles from stns 3 and 97, and were transferred to our sampling bottles; this seems improbable, given that duplicate $\Delta^{14}C$ and $\delta^{13}C$ analyses from the same niskin water were ±4‰ and ±0.2‰, respectively (see Section 2). An estimate of the amount of surface POC that could account for increases in $\Delta^{14}C$ (−442‰ at stn 3, –475‰ at stn 97) are made assuming surface $\Delta^{14}C$ of POC was 25‰ in 2018 (Hansmann & Sonnerup, 2022) at both locations, and a deep DOC $\Delta^{14}C$ average of −500‰. We calculate that 5% and 10% modern POC would need to have been dissolved to DOC at stn 97 and stn 3 to increase their $\Delta^{14}C$ to −475‰ and −446‰, respectively. A 5%–10% shift in DOC concentration is 2–4 μM, which is >2 sigma of the error of our concentration values (±0.6 μM).

Of note is that the Arabian Sea is a significant OMZ in the North Indian, and we pose the question of whether this region could contribute young and/or old DOC to the deep water. Presently, little information is available as to how OMZs affect [DOC] and DOC cycling. Rixen et al. (2010) estimate that the Arabian Sea and the Gulf of Bengal have 21% of the total volume of oxygen depleted ocean waters, though our stations were outside of the limits of the Arabian Sea OMZ (lowest oxygen concentration was 25 μmol/kg at stn 97, 700 m). It remains an open question whether processes that occur in OMZs (annamox, denitrification, chemosynthesis) contribute to changes in the cycling of DOC in the Arabian Sea or the Bay of Bengal.

Second, the presence of a contaminant whose $\delta^{13}C$ is lower than that of oceanic DOC (e.g., oil) likely did not occur in the four samples from stn 3 (Figure 3), because [DOC] would have been significantly higher in these samples than in those from surrounding seawater. We see no differences between [DOC] in the samples with low $\Delta^{14}C$ or those with low $\delta^{13}C$ than those of other samples from similar depths (Druffel, 2023).

Third, input of low $\delta^{13}C$ DOC to the deep ocean, such as that associated with on and off-axis hydrothermal vent fluids may be occurring in the Indian Ocean, where hydrothermal ridge and flank systems are abundant, particularly near stn 3 and stn 97. Lang et al. (2006) reported chemosynthesis of DOC in ridge and flank basalts, and McCarthy et al. (2011) found low $\Delta^{14}C$ and low $\delta^{13}C$ in DOC emanating from ridge-flank and on-axis hydrothermal fluids in the northeastern Pacific. Thus, it is possible that DOC produced in hydrothermal flanks and ridge systems is present and responsible for lowering of DOC $\Delta^{14}C$ and $\delta^{13}C$.

4.4. Surface DOC $\delta^{13}C$ Versus Temperature

Surface ocean DOC $\delta^{13}C$ (from 3 to 20 m depth) and SST of the water samples from the I07N cruise show similar correlation to those obtained from the Pacific and Southern oceans (Druffel et al., 2019, 2021) (Figure S3 in

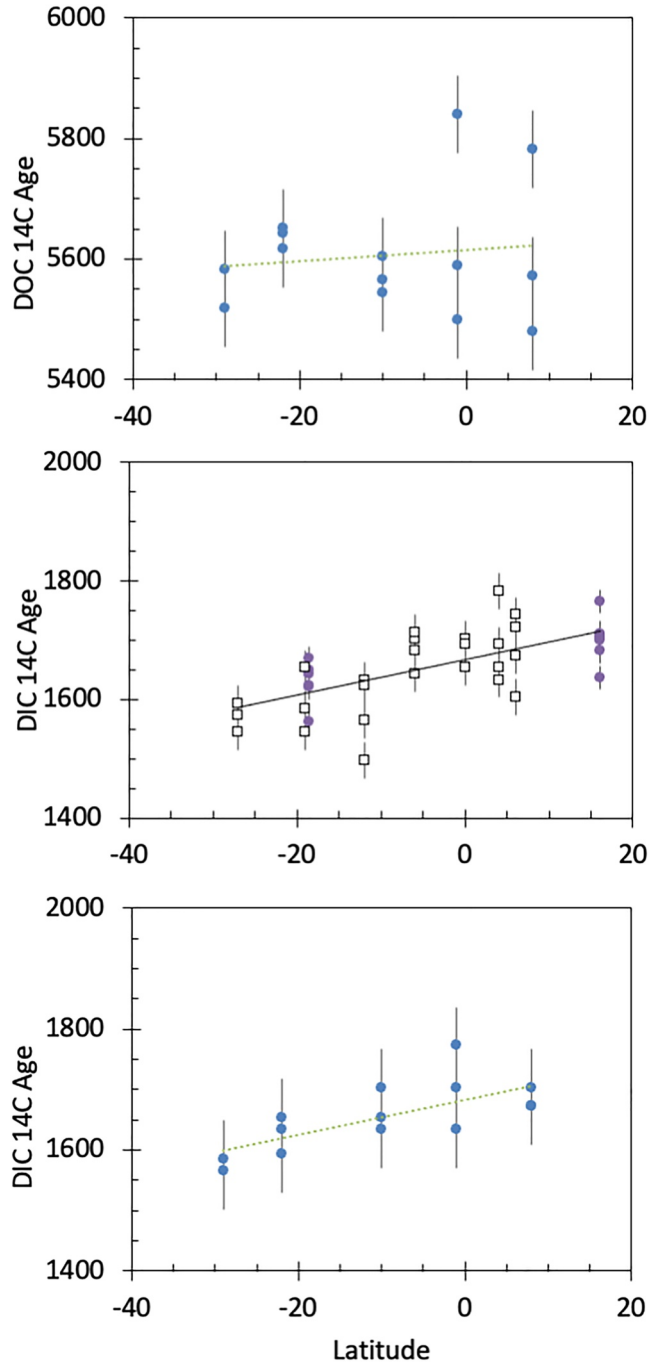

Figure 4. (a) Dissolved organic carbon ^{14}C age versus latitude from 5 stations on the I07N cruise in the west Indian in 2018 for samples with sigma4 45.75–45.80 (Circumpolar Deep Water (CDW)). The line is the Model II geometric mean regression of all points, with equation (0.95 ± 2.0) • x + 5,620 ± 34 (r^2 = 0.02). (b) Dissolved inorganic carbon (DIC) ^{14}C age versus latitude from two stations on the I07N cruise in 1995 (purple circles, Key & Quay, 2002), and 7 Geosecs stations between 27°S and 16°N in 1977–1978 (white squares, Stuiver & Ostlund, 1983) for samples with sigma4 45.75–45.80 (CDW). The line is the Model II geometric mean regression with equation y = (3.01 ± 0.54) • x + 1,667 ± 8 (r^2 = 0.44). (c) DIC ^{14}C age versus latitude from the I07N 2018 cruise (Hansmann & Sonnerup, 2022). The line is the Model II geometric mean regression with equation y = (2.90 ± 0.83) • x + 1,683 ± 13 (r^2 = 0.50).

Supporting Information S1). However, there is a relatively small range of SST for the I07N samples (23–29°C), due to the short latitudinal range of the stations (29°S–8°N), compared to the large range of SST from the Pacific and Southern oceans (0–26°C, 69°S–20°N) (Figure S3 in Supporting Information S1).

Rau et al. (1989) reported that $\delta^{13}C$ of surface plankton was correlated with SST, and that the variability of surface plankton $\delta^{13}C$ was due to carbon isotopic fractionation caused by variable concentration of aqueous CO_2 in seawater. The similarity of plankton $\delta^{13}C$ with DOC $\delta^{13}C$ indicates that surface primary producers are a main component of DOC in the surface ocean. The similarity of DOC $\delta^{13}C$ with plankton $\delta^{13}C$ provides an important end-member in the two-component mixing model of marine DOC, where surface waters are believed to be a mixture of recently produced DOC and a background of old, refractory carbon (Beaupré et al., 2020).

5. Implications for the DOC Cycle and Future Work

We show that the aging of DOC and DIC northward in the deep subtropical and equatorial West Indian Ocean are dissimilar, unlike those observed previously for the central and East Pacific (Druffel et al., 2019, 2021). This indicates that there are processes affecting the isotopic signatures of deep DOC in the Indian that are unlike those controlling DIC circulation in the deep global ocean.

A large fraction of the DOC in the deep ocean is refractory (Hansell, 2013), however, in the West Indian Ocean, there may be significant input of young DOC from dissolution of surface-derived POC. The North Indian Ocean contains a large OMZ that is maintained, in part, by large fluxes of POC into the deep ocean. There were only two samples from the Indian that had low $\Delta^{14}C$ values (−513‰, 517‰), fewer than those found in the deep Pacific that suggested evidence of ancient DOC produced in hydrothermal ridge systems (Druffel et al., 2021). Locations similar to the Indian Ocean, where there are hydrothermal systems present throughout, may be swamped by large amounts of young DOC that is formed, possibly as a result of OMZ systems.

Conflict of Interest

The authors declare no conflicts of interest relevant to this study.

Data Availability Statement

Data from the I07N cruise are available in Druffel (2023) and at the CCHDO Data Center at https://cchdo.ucsd.edu/cruise/33RO20180423 using the expocode 33RO20180423.

Acknowledgments
We thank Jennifer Walker, Xiaomei Xu, and Hector Martinez De La Torre for the stable carbon isotope measurements, John Southon and staff for their assistance and advice, chief scientists Denis Volkov and Viviane Menezes, and Jim Swift for shared ship time. This work was supported by NSF (OCE-1458941 and OCE-1951073 to E.R.M.D.), Fred Kavli Foundation, Keck Carbon Cycle AMS Laboratory, NSF/NOAA funded GO-SHIP Program, and Canada Research Chairs program (to B. D. W.).

References

Amon, R. M. W., & Benner, R. (1996). Bacterial utilization of different size classes of dissolved organic matter. *Limnology & Oceanography*, *41*(1), 41–51. https://doi.org/10.4319/lo.1996.41.1.0041

Beaupré, S. R., & Druffel, E. R. M. (2009). Constraining the propagation of bomb-radiocarbon through the dissolved organic carbon (DOC) pool in the northeast Pacific Ocean. *Deep-Sea Research I*, *56*(10), 1717–1726. https://doi.org/10.1016/j.dsr.2009.05.008

Beaupré, S. R., Druffel, E. R. M., & Griffin, S. (2007). A low-blank photochemical extraction system for concentration and isotopic analyses of marine dissolved organic carbon. *Limnology and Oceanography: Methods*, *5*(6), 174–184. https://doi.org/10.4319/lom.2007.5.174

Beaupré, S. R., Walker, B. D., & Druffel, E. R. M. (2020). The two–component model coincidence: Evaluating the validity of marine dissolved organic radiocarbon as a stable–conservative tracer at Station M. *Deep-Sea Research II*, *173*, 104737. https://doi.org/10.1016/j.dsr2.2020.104737

Benner, R., & Amon, R. M. W. (2015). The size reactivity continuum of major bioelements in the ocean. *Annual Review of Marine Science*, *7*(1), 185–205. https://doi.org/10.1146/annurev-marine-010213-135126

Bercovici, S. K., McNichol, A. P., Xu, L., & Hansell, D. A. (2018). Radiocarbon content of dissolved organic carbon in the South Indian Ocean. *Geophysical Research Letters*, *45*(2), 872–879. https://doi.org/10.1002/2017GL076295

Bien, G., Rakestraw, N. W., & Suess, H. E. (1965). Radiocarbon in the Pacific and Indian Oceans and its relation to deep water movements. *Limnology & Oceanography*, *10*(suppl), R25–R37. https://doi.org/10.4319/lo.1965.10.suppl2.r25

Broecker, W. S., Gerard, R., Ewing, M., & Heezen, B. C. (1960). Natural radiocarbon in the Atlantic Ocean. *Journal of Geophysical Research*, *65*(9), 2903–2931. https://doi.org/10.1029/jz065i009p02903

Bullister, J. (2018). Cruise report for the 2018 US GO-SHIP reoccupation of I07N section. Expedition 33RO20180423. Retrieved from https://cchdo.ucsd.edu/cruise/33RO20180423

Cherrier, J., Bauer, J. E., Druffel, E. R. M., Coffin, R., & Chanton, J. (1999). Radiocarbon in marine bacteria: Evidence for the ages of assimilated carbon. *Limnology & Oceanography*, *44*(3), 730–736. https://doi.org/10.4319/lo.1999.44.3.0730

Druffel, E. R. M. (2023). DOC ^{14}C and ^{13}C data from Cruise 33RO20180423, exchange version [Dataset]. CCHDO. https://cchdo.ucsd.edu/cruise/33RO20180423

Druffel, E. R. M., Griffin, S., Coppola, A. I., & Walker, B. D. (2016). Radiocarbon in dissolved organic carbon of the Atlantic Ocean. *Geophysical Research Letters*, *43*(10), 5279–5286. https://doi.org/10.1002/2016GL068746

Druffel, E. R. M., Griffin, S., Garcia, N. G., Wang, N., McNichol, A. P., Key, R., & Walker, B. W. (2019). Dissolved organic radiocarbon in the central Pacific Ocean. *Geophysical Research Letters*, *46*(10), 5396–5403. https://doi.org/10.1029/2019GL083149

Druffel, E. R. M., Griffin, S., Lewis, C. B., Rudresh, M., Garcia, N. G., Key, R. M., et al. (2021). Dissolved organic radiocarbon in the eastern Pacific and Southern Oceans. *Geophysical Research Letters*, *48*(10), e2021GL092904. https://doi.org/10.1029/2021GL092904

Estes, E. S., Berti, D., Coffey, N. R., Hochella, M. F., Wozniak, A. S., & Luther, G. W. (2019). Abiotic synthesis of graphite in hydrothermal vents. *Nature Geoscience*, *10*(1), 5179. https://doi.org/10.1038/s41467-019-13216-z

Hansell, D. A. (2013). Recalcitrant dissolved organic carbon fractions. *Annual Review of Marine Science*, *5*(1), 421–445. https://doi.org/10.1146/annurev-marine-120710-100757

Hansmann, R., & Sonnerup, R. (2022). *Data from GO-SHIP I07N cruise using the expocode 33RO20180423*. CCHDO Data Center. Retrieved from https://cchdo.ucsd.edu/cruise/33RO20180423

Jiao, N., Herndl, G. J., Hansell, D. A., Benner, R., Kattner, G., Wilhelm, S. W., et al. (2010). Microbial production of recalcitrant dissolved organic matter: Long-term carbon storage in the global ocean. *Nature Reviews Microbiology*, *8*, 589–599. https://doi.org/10.1038/nrmicro2386

Kaiser, K., & Benner, R. (2009). Biochemical composition and size distribution of organic matter at the Pacific and Atlantic time-series stations. *Marine Chemistry*, *113*(1–2), 63–77. https://doi.org/10.1016/j.marchem.2008.12.004

Key, R. M., & Quay, P. (2002). *U.S. WOCE Indian Ocean survey: Final report for radiocarbon*. Ocean Tracer Laboratory; Technical Report 02-1.

Lang, S. Q., Butterfield, D. A., Lilley, M. D., Johnson, H. P., & Hedges, J. I. (2006). Dissolved organic carbon in ridge-axis and ridge-flank hydrothermal systems. *Geochimica et Cosmochimica Acta*, *70*(15), 3830–3842. https://doi.org/10.1016/j.gca.2006.04.031

Mantyla, A. W., & Reid, J. L. (1995). On the origins of deep and bottom waters of the Indian Ocean. *Journal of Geophysical Research*, *100*(C2), 2417–2439. https://doi.org/10.1029/94JC02564

McCarthy, M., Beaupré, S., Walker, B., Voparil, I., Guilderson, T., & Druffel, E. (2011). Chemosynthetic origin of ^{14}C-depleted dissolved organic matter in a ridge-flank hydrothermal system. *Nature Geoscience*, *4*(1), 32–36. https://doi.org/10.1038/ngeo1015

Mopper, K., Zhou, X., Kieber, R. J., Kieber, D. J., Sikorski, R. J., & Jones, R. D. (1991). Photochemical degradation of dissolved organic carbon and its impact on the oceanic carbon cycle. *Nature*, *353*(6339), 60–62. https://doi.org/10.1038/353060a0

Rau, G. H., Takahashi, T., & Des Marias, D. J. (1989). Latitudinal variations in plankton δ^{13}C: Implications for CO_2 and productivity in past oceans. *Nature*, *341*(6242), 516–518. https://doi.org/10.1038/341516a0

Rixen, T., Cowie, G., Gaye, B., Goes, J., Rosario Gomes, H. D., Hood, R. R., et al. (2010). Present, past and future of the OMZ in the northern Indian Ocean. *Biogeosciences Discussions*, *82*(2), 19. https://doi.org/10.5194/bg-2020-82

Santos, G. M., Southon, J. R., Drenzek, N. J., Ziolkowski, L., Druffel, E. R. M., Xu, X., et. al. (2010). Blank assessment for ultra–small radiocarbon samples: Chemical extraction and separation vs. AMS. *Radiocarbon*, *52*(3), 1322–1335. https://doi.org/10.1017/s0033822200046415

Smith, D. C., Simon, M., Alldredge, A. L., & Azam, F. (1992). Intense hydrolytic enzyme activity on marine aggregates and implications for rapid particle dissolution. *Nature*, *359*(6391), 139–142. https://doi.org/10.1038/359139a0

Smith, S. L. (2001). Understanding the Arabian Sea: Reflections on the 1994–1996 Arabian Sea expedition. *Deep Sea Research II*, *48*(6–7), 1385–1402. https://doi.org/10.1016/s0967-0645(00)00144-2

Srinivasan, A., Rooth, C. G. H., Top, Z., & Olson, D. B. (2000). Abyssal upwelling in the Indian Ocean: Radiocarbon diagnostics. *Journal of Marine Research*, *58*(5), 755–778. https://doi.org/10.1357/002224000321358891

Stuiver, M., & Ostlund, H. G. (1983). GEOSECS Indian Ocean and Mediterranean radiocarbon. *Radiocarbon*, *25*(1), 1–29. https://doi.org/10.1017/s0033822200005270

Stuiver, M., & Polach, H. A. (1977). Discussion: Reporting of ^{14}C data. *Radiocarbon*, *19*(3), 355–363. https://doi.org/10.1017/s0033822200003672

Stuiver, M., Quay, P. D., & Ostlund, H. G. (1983). Abyssal water ^{14}C distribution and the age of the world oceans. *Science*, *219*(4586), 849–851. https://doi.org/10.1126/science.219.4586.849

Talley, L. D. (2013). Hydrographic Atlas of the World Ocean circulation experiment (WOCE). In M. Sparrow, P. Chapman, & J. Gould (Eds.), *Volume 4: Indian Ocean*. International WOCE Project Office.

Toggweiler, J. R., Dixon, K., & Bryan, K. (1989a). Simulations of radiocarbon in a coarse-resolution World Ocean model. Steady state pre-bomb distributions. *Journal of Geophysical Research*, *94*(C6), 8217–8242. https://doi.org/10.1029/jc094ic06p08217

Toggweiler, J. R., Dixon, K., & Bryan, K. (1989b). Simulations of radiocarbon in a coarse-resolution World Ocean model 2. Distributions of bomb-produced carbon 14. *Journal of Geophysical Research*, *94*(C6), 8243–8264. https://doi.org/10.1029/jc094ic06p08243

Walker, B. D., Beaupré, S. R., Griffin, S., & Druffel, E. R. M. (2019). UV photochemical oxidation and extraction of marine dissolved organic carbon at UC Irvine: Status, surprises, and methodological recommendations. *Radiocarbon*, *61*(5), 1603–1617. https://doi.org/10.1017/RDC.2019.9

Walker, B. D., & Xu, X. (2019). An improved method for the sealed-tube zinc graphitization of microgram carbon samples and ^{14}C AMS measurement. *Nuclear Instruments & Methods in Physics Research Section B-Beam Interactions with Materials and Atoms*, *438*, 58–65. https://doi.org/10.1016/j.nimb.2018.08.004

Walker, B. W., Beaupré, S. R., Guilderson, T. P., McCarthy, M. D., & Druffel, E. R. M. (2016). Pacific carbon cycling constrained by organic matter size, age and composition relationships. *Nature Geoscience*, *9*(12), 888–891. https://doi.org/10.1038/ngeo2830

Williams, P. M., & Druffel, E. R. M. (1987). Radiocarbon in dissolved organic carbon in the central North Pacific Ocean. *Nature*, *330*(6145), 246–248. https://doi.org/10.1038/330246a0

Xu, X., Trumbore, S. E., Zheng, S., Southon, J. R., McDuffee, K. E., Luttgen, M., & Liu, J. C. (2007). Modifying a sealed tube zinc reduction method for preparation of AMS graphite targets: Reducing background and attaining high precision. *Nuclear Instruments and Methods in Physics Research B*, *259*(1), 320–329. https://doi.org/10.1016/j.nimb.2007.01.175

References From the Supporting Information

Volkov, D. (2018). Cruise report for the 2018 US GO-SHIP reoccupation of I07N section. Expedition 33RO20180423. Retrieved from https://cchdo.ucsd.edu/cruise/33RO20180423